Measurement of Gamma Rays from Laser-Electron Collisions in ZEUS TA1

Paul S Gellersen[1], Christopher Arran[2], Elias Gerstmayr[3], Hannah Jager[3], Brendan Kettle[4], Owen Lawrence[1], Eva Los[5], Yong Ma[6], Stuart Mangles[4], Conor McAnespie[3], Christopher Ridgers[1], Gianluca Sarri[3], Matthew Streeter[3], Christopher D Murphy[1]

[1]**University of York, York, UK**
[2]**Lancaster University, Bailrigg, Lancaster, UK**
[3]**Queen's University Belfast, University Road, Belfast, UK**
[4]**Imperial College London, London, UK**
[5]**University of Oxford, Oxford, UK**
[6]**University of Michigan, Ann Arbor, MI, United States**

Abstract

ZEUS offers access to new regimes of strong-field QED via collisions of GeV-scale electron beams, generated by laser-wakefield acceleration, with intense laser pulses. In these collisions gamma rays are produced by non-linear inverse Compton scattering, and diagnosis of these provides insight into the strong-field interaction. Typically the gamma rays spectral distribution is diagnosed by measuring energy deposition in a crystal as a function of depth, and their angular distribution by imaging the spatial profile of energy deposition in a crystal. Reconstructing the true distributions from these measurements requires deconvolving the energy-dependent response function, usually by assuming some shape to the energy spectrum and optimising free parameters such that the calculated response best matches the data. Here we describe a recent collision experiment in ZEUS TA1, how the gamma rays are diagnosed and some preliminary results, the calculation of the response functions, and propose optimisation of a forward model of the collisions as an alternative way to reconstruct gamma ray distributions, without any assumption of shape.

Introduction

In electromagnetic fields of strength comparable to the Schwinger field $E_{sch} = 1.3 \times 10^{18}\,\mathrm{V\,m^{-1}}$ (termed strong fields) the theory of QED breaks down, and we must apply the Furry picture of strong-field QED (SFQED) instead [1, 2]. Strong fields exist around certain astrophysical objects, such as pulsars [3] and magnetars [4], close to high-Z nuclei [5], and are expected at the interaction point of next-generation collider experiments [6]. However, creating them in well-controlled experiments is challenging, and so the theory of SFQED remains largely untested. One successful approach has been to collide high-energy electron beams (produced by a LINAC or by laser-wakefield acceleration) with intense laser beams [7, 8, 9, 10, 11, 12, 13], in which the laser fields are relativistically upshifted to be comparable to E_{sch} in the frame of the electrons. In this type of interaction the physics is determined by two parameters: the quantum parameter $\chi_e = \frac{\gamma|\boldsymbol{E}+\boldsymbol{v}\times\boldsymbol{B}|}{E_{sch}}$, which compares the field strength in the frame of the particle to the Schwinger field; and the classical non-linearity parameter $a_0 = \frac{eE_0}{m_e c\omega}$, which represents the effective number of photons involved in a QED event [2], and is also a measure of the laser intensity. ZEUS at full power is expected to achieve $\chi_e \sim 1$ and $a_0 \sim 50$, allowing testing of physics models in a regime of SFQED that has not yet been reported.

In the interaction of an electron beam with a laser the most significant effect is non-linear inverse Compton scattering, in which many laser photons are absorbed by an electron, before emission of a single high-energy photon, typically in the region of 10s of MeV. For $a_0 >> 1$, the interaction of a given electron energy γ with a field of intensity a_0 and photon energy E_l produces a synchrotron spectrum with critical energy $E_{cr} \approx 3a_0^3 \frac{\gamma^2 E_l}{1+a_0^2/2}$, and the number of scattered photons scales with Na_0, where N is the number of colliding electrons [14]. The spectrum deviates from this for intermediate a_0 values, and in a real collision there is a distribution of electron γ values interacting with a distribution of a_0 values (laser intensity varies spatially and temporally), and so the total spectrum may deviate significantly from a synchrotron shape.

The gamma rays are emitted within a cone of angle $\frac{1}{\gamma}$ around the emitting electron's velocity vector due to the relativistic beaming effect [15], though the angular distribution integrated over a collision with a linearly-polarised laser typically appears elliptical due to the oscillation of electrons in the laser field. The extent of the elliptical shape can therefore be related to the laser intensity, under certain assumptions [16, 17].

Gamma rays are often diagnosed by a pair of scintillators; a thin profiler to measure the angular distribution, and a deep spectrometer to measure the energy deposition as a function of penetration depth. Knowing the energy-dependent response function of the spectrometer, one can fit a spectrum of some assumed shape to the measurement. A synchrotron-like shape is usually assumed, based on the assumption that the highest values of γ and a_0 dominate the emission. The profiler scintillation is also usually assumed to represent the number-weighted angular distribution, i.e. to have an energy-independent response and to emit light from a single plane. Here we propose instead assuming a forward model of the collision and scintillator responses and taking the true distributions as those output by the model when its input parameters have been optimised to reproduce the measured signals. This corresponds to replacing the above assumptions with assumptions that simulations of SFQED effects in the collision and of energy deposition in the scintillators are accurate. We can also compare the success of this process with different models (e.g. classical radiation reaction vs quantum radiation reaction) to quantitatively measure their agreement with the experimental data, similarly to [10].

The gamma rays produced inside the laser pulse may also interact with the strong field to undergo the non-linear Breit-Wheeler process, to produce electron-positron pairs [18, 19]. This is exponentially suppressed for $\chi_e < 1$ and has not yet been reported in all-optical experiments. The experiment reported here was aiming to measure the produced positrons, but it is not the subject of this article.

Experiment

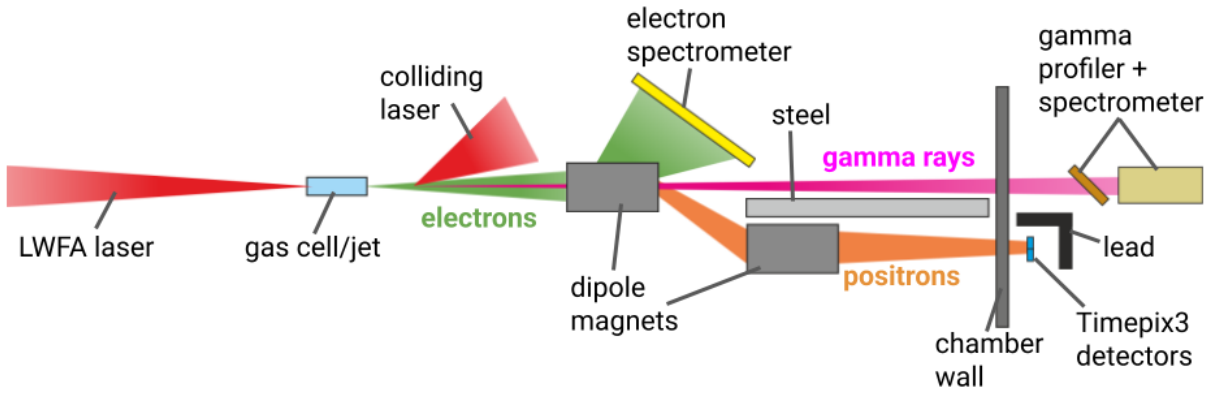

Figure 1: Experimental set-up.

The experimental set-up is shown in Figure 1. All values reported are those estimated for the set of shots presented after. The LWFA drive laser was focused at f/64 and delivered approximately 28.7 J in 27 fs to target. The target was a gas cell backed by a 1.65 bar mix of 98% He and 2% N. The electrons produced were diagnosed by magnetic deflection electron spectrometry.

The colliding laser was focused at f/3 at a 15° angle to the electrons at a point 137 mm downstream from the end of the gas. At this distance downstream the electron beam has expanded to a transverse width of order 100 µm, giving us a larger target to hit and an interaction likely to include the full laser envelope but only a small fraction of the electrons. It delivered approximately 5.7 J in 27 fs to the collision, where gamma rays and positrons are produced by inverse Compton scattering and the Breit-Wheeler process respectively.

The gamma rays were diagnosed by a profiler and spectrometer outside the vacuum chamber. The profiler was a 6 mm thick LYSO crystal, and the spectrometer was a stack of 5 x 5 x 50 mm CsI:Tl crystals (30 x 5 mm thick layers along the beam axis, each layer made up of 8 crystals stacked along each transverse axis alternately, and all held in a nylon frame and separated by rubber spacers).

The positrons were collected and guided by dipole magnets as shown onto TimePix3 single pixel silicon tracking detectors.

Measurements

In one run of 105 shots, we estimate we achieved 33 successful collisions (31.4% hit rate), based on observing low-divergence and highly penetrating gamma ray signals on the profiler and spectrometer.

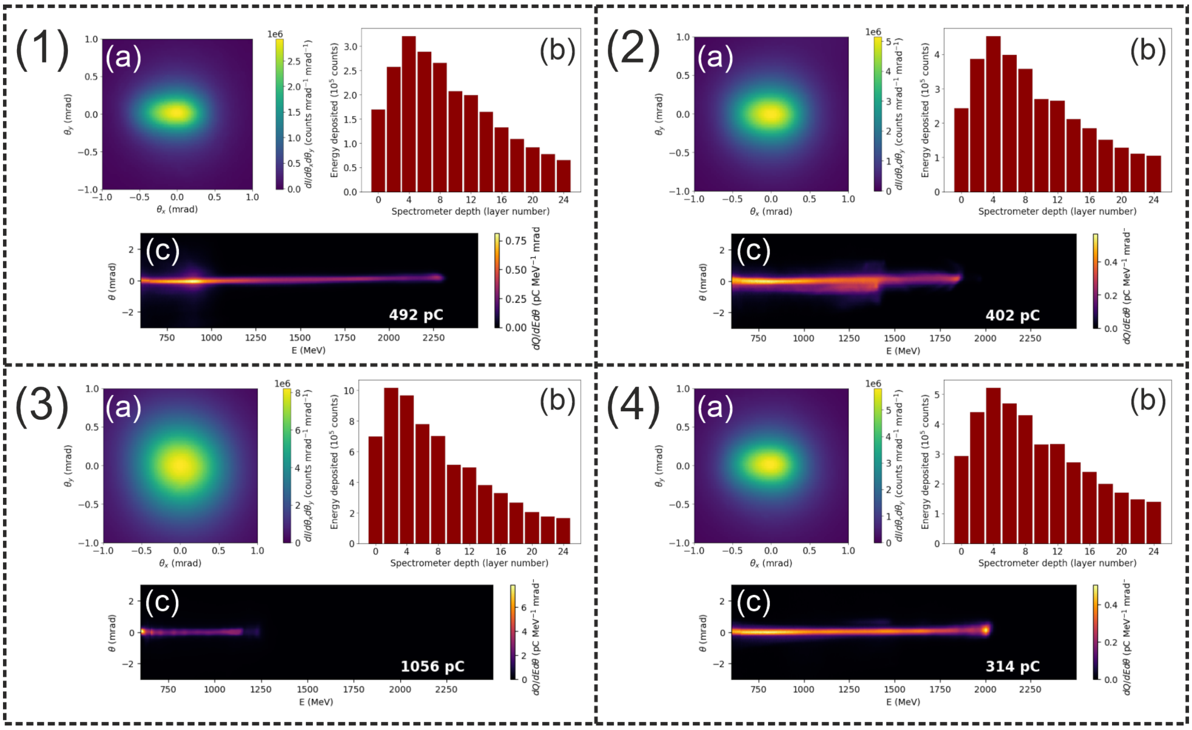

Figure 2: Measurements for four of the brightest collision shots from a single run, numbered (1)-(4). For each (a) shows the gamma ray angular distribution measured by the profiler, (b) shows the energy deposition measured by the spectrometer, and (c) shows the electron energy spectrum and divergence measured by the magnetic deflection spectrometer.

Figure 2 shows the (a) gamma ray angular distributions, (b) gamma ray spectrometer signals, and (c) electron spectra measured for 4 of the brightest collisions from this run. In this run the LWFA process consistently produced broad spectrum beams of energy up to 2.3 GeV, with 100s pC charge above 600 MeV, and <1 mrad divergence.

We can identify qualitative trends immediately by comparing shot 3 to the rest. We clearly see a less penetrating signal in the spectrometer in (3b), indicating the gamma rays were lower energy. This is consistent with the lower energy electrons seen in (3c) and less elliptical profile seen in (3a), indicating a lower laser a_0, since the scattered gamma ray energy scales as $a_0\gamma^2$. The integrated counts on the gamma diagnostics are however higher, despite scaling as $Na_0^2\gamma^2$, but this can be explained by a higher interacting charge.

Modelling of gamma ray diagnostics

To develop a more quantitative understanding of these measurements we require the energy-dependent diagnostic response functions. To build these, a model was constructed using OpenTOPAS, a code built using the GEANT4 simulation toolkit for Monte-Carlo simulations of interactions of particles with matter [20, 21]. The model is shown in Figure 3 and contains all materials along the gamma ray beam path from the collision point to the diagnostics along z.

Photons of a single energy and no angular momentum were propagated from the collision point through this set-up, and the energy deposition in the two diagnostics recorded. The energy deposition in the profiler was spatially binned along the y and z axes with a resolution of 0.06 mm per bin to produce a response like the imaging camera would record on experiment. The resolution was chosen to be twice the experimental resolution to ensure that is the limiting resolution. For each energy 1000000 photons were simulated to obtain the mean energy deposition per photon in each bin and crystal with a standard error.

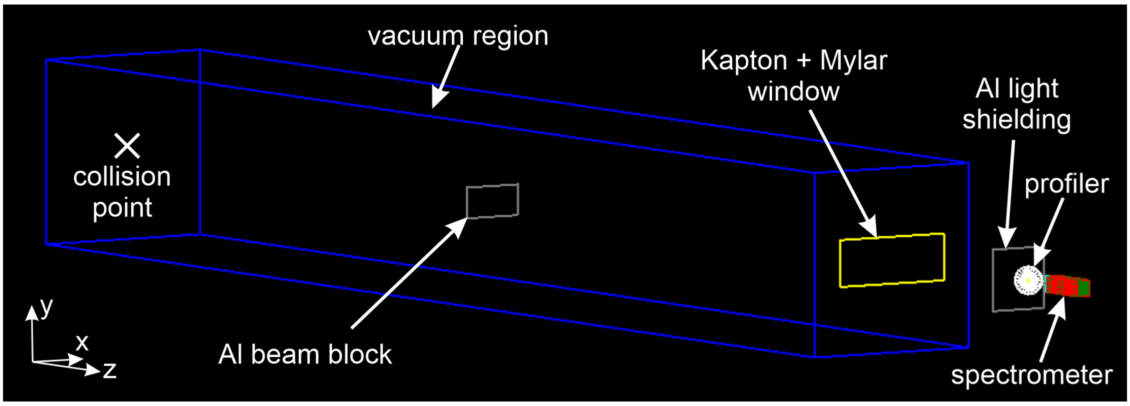

Figure 3: To-scale diagram of the included materials in the OpenTOPAS calibration simulations.

Figure 4 shows (a) the energy deposition as a function of energy and depth in the spectrometer, integrated over the transverse crystals of each layer, (b) the energy deposition as a function of energy and θ_x in the profiler, integrated over θ_y, and (c) the energy deposition as a function of energy and θ_y in the profiler, integrated over θ_x. θ_x and θ_y are the angles to the beam axis along each transverse axis.

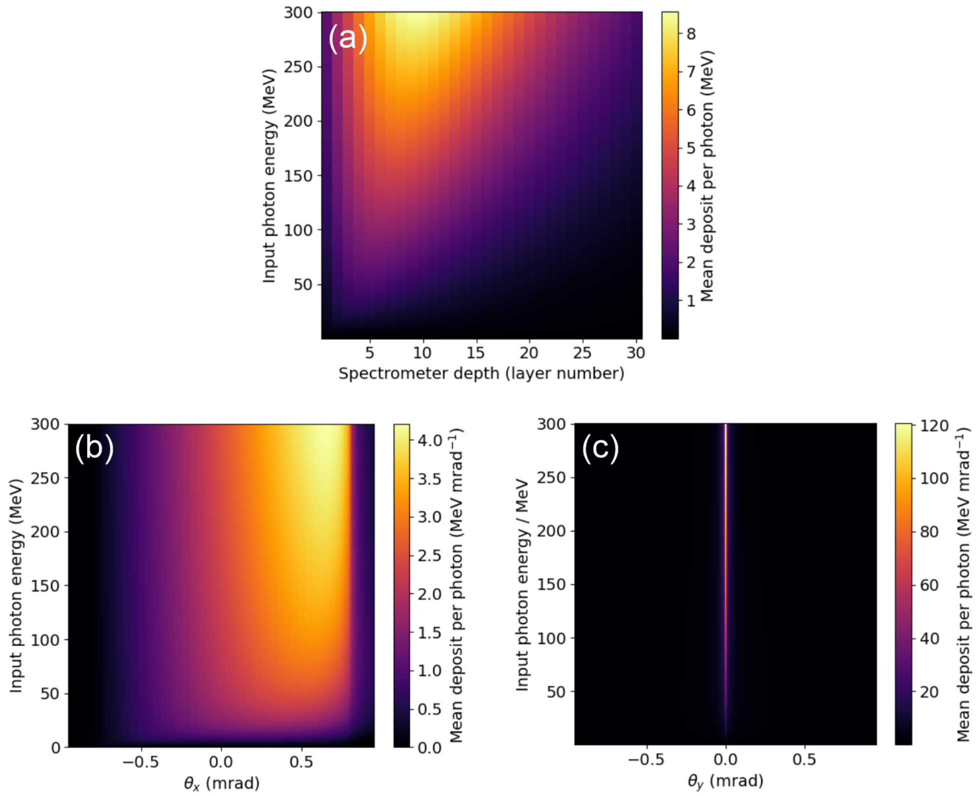

Figure 4: The energy dependent response functions of the gamma ray diagnostics. (a) is the energy deposition as a function of energy and depth in the spectrometer, integrated over the transverse crystals of each layer, (b) is the energy deposition as a function of energy and θ_x in the profiler, integrated over θ_y, and (c) is the energy deposition as a function of energy and θ_y in the profiler, integrated over θ_x

As expected we see higher total deposition the higher energy the incident photon energy in both diagnostics. (a) shows that for higher photon energies the peak deposit occurs deeper into the stack and is more spread out, as expected. (b) shows that the deposition by a photon in the profiler is spread across roughly a 1.4 mrad range along θ_x, corresponding to deposition along the path it takes through the crystal. (c) however shows that the deposition is well-localised along θ_y for all energies. The usual assumptions that the profiler response is energy-independent and is localised to a single plane of the crystal are clearly broken, hence the need for a more thorough reconstruction technique.

Proposed modelling of collisions for distribution reconstruction

Using the above response functions we can reconstruct the expected measurements for any given distribution of photons by summing the response for each photon's energy placed at its calculated incidence location. To calculate the photon distribution produced by collisions we use ptarmigan, a Monte-Carlo SFQED code for electron beams interacting with lasers [22, 23, 24]. For example, Figure 5 shows the calculated responses for the collision at 15 °of an electron beam sampled from the spectrum measured for shot (1) of Figure 2, with a Gaussian laser pulse of peak $a_0 = 2.6$, beam radius 4 µm and pulselength 27 fs. Arbitrarily chosen spatial and temporal offsets of 48.3 and 11.5 µm were used.

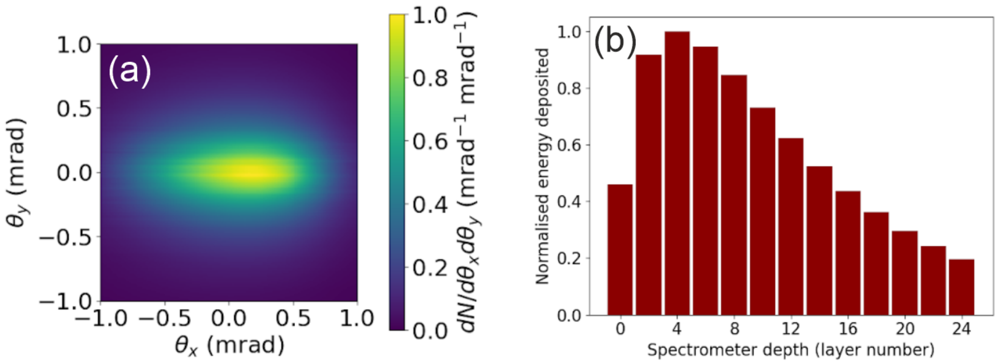

Figure 5: The calculated profiler and spectrometer measurements for an example collision with arbitrarily chosen parameters, reconstructed using the response matrices in Figure 4.

The reconstructed profile appears slightly streaky because the Monte-Carlo sampling of the collision produces a non-smooth distribution of gamma rays, and the response per photon is spread across a θ_x range, as shown in Figure 4 (b). To find simulations that match our measurements, we propose an iterative loop in which a set of input collision parameters are optimised such that the reconstructed response best matches the measurements. Multiple simulations can be run with the same parameters to estimate the uncertainties due to sampling, which allow better fitting and optimisation of parameters. Allowing too many parameters to be optimised is computationally expensive and may cause over-fitting, so a limited set should be chosen of those that vary the most experimentally and have the largest non-degenerate effect on the resulting distribution. This choice is the subject of current work. The result of this process is a best-fit simulation that provides us the full photon distribution with no assumptions of its form except that the physics models in ptarmigan are accurate and any assumptions made to fix collision parameters.

Conclusions

We have described a recent experiment in ZEUS TA1 to measure effects of strong-field QED in collisions of high energy electron beams generated by laser-wakefield acceleration and intense laser pulses, presented some measurements of gamma ray signals in successful collisions, and proposed a new method for determining the full gamma ray distribution. The measured gamma rays follow expected qualitative trends, but quantitative analysis is limited by the large number of unknown collision parameters, and the energy-dependent response functions of the diagnostics. We presented our method of determining these response functions by OpenTOPAS simulations, which then allow calculation of the expected measurement for any given gamma ray distribution. Finally we explained how an iterative loop of collision simulations, measurement reconstruction and comparison to a real measured signal to find the best-fit simulation provides the full photon distribution without any assumption of shape.

Acknowledgements

We would like to thank the entire team at the ZEUS laser facility for their work on this experiment. The Viking cluster was used during this project, which is a high performance compute facility provided by the University of York. We are grateful for computational support from the University of York, IT Services and the Research IT team.

References

[1] WH Furry. On bound states and scattering in positron theory. *Physical Review*, 81(1):115, 1951.

[2] A Gonoskov, TG Blackburn, M Marklund, and SS Bulanov. Charged particle motion and radiation in strong electromagnetic fields. *Reviews of Modern Physics*, 94(4):045001, 2022.

[3] Alice K Harding and Dong Lai. Physics of strongly magnetized neutron stars. *Reports on Progress in Physics*, 69(9):2631–2708, 2006.

[4] RP Mignani, Vincenzo Testa, D González Caniulef, Roberto Taverna, Roberto Turolla, S Zane, and K Wu. Evidence for vacuum birefringence from the first optical polarimetry measurement of the isolated neutron star rx j1856. 5- 3754. *Monthly Notices of the Royal Astronomical Society*, page stw2798, 2016.

[5] AI Milstein and Martin Schumacher. Present status of delbrück scattering. *Physics reports*, 243(4):183–214, 1994.

[6] V Yakimenko, S Meuren, F Del Gaudio, C Baumann, A Fedotov, F Fiuza, T Grismayer, MJ Hogan, A Pukhov, LO Silva, et al. Prospect of studying nonperturbative qed with beam-beam collisions. *Physical review letters*, 122(19):190404, 2019.

[7] DL Burke, RC Field, G Horton-Smith, JE Spencer, D Walz, SC Berridge, WM Bugg, K Shmakov, AW Weidemann, C Bula, et al. Positron production in multiphoton light-by-light scattering. *Physical Review Letters*, 79(9):1626, 1997.

[8] C Bula, Kirk T McDonald, Eric J Prebys, Charles Bamber, Steven Boege, Theofilos Kotseroglou, Adrian C Melissinos, David D Meyerhofer, W Ragg, David L Burke, et al. Observation of nonlinear effects in compton scattering. *Physical Review Letters*, 76(17):3116, 1996.

[9] JM Cole, KT Behm, E Gerstmayr, TG Blackburn, JC Wood, CD Baird, Matthew J Duff, C Harvey, A Ilderton, AS Joglekar, et al. Experimental evidence of radiation reaction in the collision of a high-intensity laser pulse with a laser-wakefield accelerated electron beam. *Physical Review X*, 8(1):011020, 2018.

[10] Eva E Los, Elias Gerstmayr, Christopher Arran, Matthew JV Streeter, Cary Colgan, Claudia C Cobo, Brendan Kettle, Thomas G Blackburn, Nicolas Bourgeois, Luke Calvin, et al. Observation of quantum effects on radiation reaction in strong fields. *Nature Communications*, 2026.

[11] Kristjan Poder, Matteo Tamburini, G Sarri, Antonino Di Piazza, S Kuschel, CD Baird, K Behm, S Bohlen, JM Cole, DJ Corvan, et al. Experimental signatures of the quantum nature of radiation reaction in the field of an ultraintense laser. *Physical Review X*, 8(3):031004, 2018.

[12] Mohammad Mirzaie, Calin Ioan Hojbota, Do Yeon Kim, Vishwa Bandhu Pathak, Tae Gyu Pak, Chul Min Kim, Hwang Woon Lee, Jin Woo Yoon, Seong Ku Lee, Yong Joo Rhee, et al. All-optical nonlinear compton scattering performed with a multi-petawatt laser. *Nature Photonics*, 18(11):1212–1217, 2024.

[13] Aimé Matheron, Jean-Raphaël Marquès, Vincent Lelasseux, Yinren Shou, Igor A Andriyash, Vanessa Ling Jen Phung, Yohann Ayoul, Audrey Beluze, Ioan Dăncuş, Fabien Dorchies, et al. Compton photons at the gev scale from self-aligned collisions with a plasma mirror. *arXiv preprint arXiv:2412.19337*, 2024.

[14] Eric Esarey, Sally K Ride, and Phillip Sprangle. Nonlinear thomson scattering of intense laser pulses from beams and plasmas. *Physical Review E*, 48(4):3003, 1993.

[15] TG Blackburn, D Seipt, SS Bulanov, and M Marklund. Radiation beaming in the quantum regime. *Physical Review A*, 101(1):012505, 2020.

[16] TG Blackburn, E Gerstmayr, SPD Mangles, and M Marklund. Model-independent inference of laser intensity. *Physical Review Accelerators and Beams*, 23(6):064001, 2020.

[17] K Fleck, T Blackburn, E Gerstmayr, M Bruschi, P Grutta, M Morandin, and G Sarri. Dependence of the number-weighted angular distribution of compton-scattered photon beams on the laser intensity. *Physical Review A*, 110(2):023510, 2024.

[18] Howard R Reiss. Absorption of light by light. *Journal of Mathematical Physics*, 3(1):59–67, 1962.

[19] AI Nikishov and VI Ritus. Quantum processes in the field of a plane electromagnetic wave and in a constant field. i. *Sov. Phys. JETP*, 19(2):529–541, 1964.

[20] B. Faddegon, J. Ramos-Mendez, J. Schuemann, A. McNamara, J. Shin, J. Perl, and Paganetti H. The TOPAS Tool for Particle Simulation, a Monte Carlo Simulation Tool for Physics, Biology and Clinical Research. *Physica Medica*, 72:114–121, 2020.

[21] J. Perl, J. Shin, J. Schumann, B. Faddegon, and H. Paganetti. TOPAS: An innovative proton Monte Carlo platform for research and clinical applications. *Medical Physics*, 39:6818, 2012.

[22] TG Blackburn, AJ MacLeod, and B King. From local to nonlocal: higher fidelity simulations of photon emission in intense laser pulses. *New Journal of Physics*, 23(8):085008, 2021.

[23] TG Blackburn and B King. Higher fidelity simulations of nonlinear breit–wheeler pair creation in intense laser pulses. *The European Physical Journal C*, 82(1):44, 2022.

[24] TG Blackburn, B King, and S Tang. Simulations of laser-driven strong-field qed with ptarmigan: Resolving wavelength-scale interference and γ-ray polarization. *Physics of Plasmas*, 30(9), 2023.